Science and Technology Indonesia
e-ISSN:2580-4391 *p*-ISSN:2580-4405
Vol. 10, No. 3, July 2025

Research Paper

Synthesis and Characterization of Polyvinyl Alcohol (PVA) Nanofiber Membranes with *Annona muricata* and *Terminalia catappa* Leaf Extract

Silfiyana Fitria[1], Muhammad Rama Almafie[2], Ihsan Alfikro[3], Fiber Monado[1], Ida Sriyanti[4], Idha Royani[5*]

[1]*Master of Physics, Faculty of Mathematics and Natural Sciences, Universitas Sriwijaya, Palembang, South Sumatera, 30139, Indonesia*
[2]*Doctoral of Mathematics and Natural Sciences, Faculty of Mathematics and Natural Sciences, Universitas Sriwijaya, Palembang, South Sumatera, 30139, Indonesia*
[3]*Laboratory of Material Science, Faculty of Mathematics and Natural Science, Universitas Sriwijaya, Indralaya, South Sumatera, 30662, Indonesia*
[4]*Master of Physics Education, Faculty of Education, Universitas Sriwijaya, Jalan Srijaya Negara, Bukit Lama, Palembang, South Sumatera, 30137, Indonesia*
[5]*Master Program of Material Science, Graduate School, Universitas Sriwijaya, Palembang, 30139, Indonesia, Indonesia*
*__Corresponding author__: idharoyani@unsri.ac.id

Abstract
Polyvinyl alcohol (PVA) is hydrophilic, flexible, elastic, and environmentally friendly, leading to the wide use as a binder in nanofiber matrices. The nanofibers of PVA are frequently combined with extract possessing antibacterial properties for characterization. Therefore, this study aimed to produce PVA nanofibers incorporating soursop leaf extract (ALE) and catappa leaf extract (CLE) using electrospinning for the investigation of the physicochemical, mechanical, and antibacterial properties. Electron microscopy showed that the electrospun nanofibers had a yellowish-brown surface with diameters ranging from 962 nm to 1323 nm. Fourier Transform Infrared (FTIR) analysis revealed the presence of functional groups interacting through hydrogen bonding, leading to a shift in wavenumbers. The tensile strength of PAC-1, PAC-2, and PAC-3 nanofibers decreased from 8.46 MPa to 4.27 MPa, followed by a reduction in Young's modulus from 20.2 MPa to 0.89 MPa. The effect of extract concentration on the reduction in tensile strength and Young's modulus was related to aggregation in certain areas of the nanofibers and weakened intermolecular polymer interactions. Pure extract had strong antibacterial activity and nanofiber membranes had moderate activity with inhibition zones ranging from 12.3 to 16.8 mm and 8.0 to 14.4 mm, respectively. The results showed that the produced fibers could be used in the biomedical field for wound dressings and filtration, as well as in textiles.

Keywords
Membranes, Soursop, Katapang, Polyvinyl Alcohol, Antibacterial

Received: 5 December 2024, Accepted: 2 May 2025
https://doi.org/10.26554/sti.2025.10.3.837-846

1. INTRODUCTION

Nanomaterials have received significant attention in various fields, including nanofibers. Superior characteristics, such as mechanical strength, large surface area, and good conductivity, are unique properties of nanofibers that provide space for numerous innovative applications (Valipouri et al., 2024). Nano- and microfibers have been synthesized using several methods (Almafie et al., 2025; Sriyanti et al., 2024), including the electrospinning process, which uses static electricity for production with the advantages of low cost (Almafie et al., 2024) as well as superior structure and morphology. Investigations on nanofibers are promising because of their capability to produce fibers with petite sizes reaching the nanometer scale with wide application in biomaterials, biotechnology, tissue engineering, and many other fields (Keirouz et al., 2023). In electrospinning, process parameters including concentration, viscosity, and voltage should be considered, as well as environmental parameters in the form of humidity, due to potential effects on the resulting nanofibers (Al-Abduljabbar and Farooq, 2023). The binder (matrix) is used to produce fine fibers and a common example is Polyvinyl Alcohol Polymer (PVA) with a molecular weight of 89,000-98,000. PVA has promising physicochemical properties, including water solubility, good mechanical strength, and applications in various fields .This polymer can dissolve in polar solvents and is highly dependent on its degree of hydrolysis (Sapalidis, 2020).

Pristine PVA polymers are widely used and can be modified with natural materials to produce nanofibers applicable in the biomedical field (Akpan et al., 2021). The use of natural materials is essential because of their ability to produce nanofibers with better characteristics compared to solitary polymers integrated with PVA and Hibiscus leaves in the fabrication of nanofibers for wound dressing applications (Sen et al., 2022).

This combination generated nanofibers with characteristics that provided protection against bacterial growth and conferred moisturizing effects on wounds, preventing itchiness caused by dryness (Gheibi et al., 2024) conducted antibacterial assays on nanofibers comprising natural extracts of *Aspergillus euchroma*, *Allium sativum*, and *Echinacea purpurea* combined with PVA, which produced a 7 mm inhibition zone against *Staphylococcus aureus* bacteria.

Current investigations are predominantly focused on the individual effects of each natural extract, whereas the potential synergistic effects of the extract combination remain largely unexplored, offering an opportunity for novel discoveries. This study presents a new combination of soursop leaf extract (ALE) and catappa leaf extract (CLE) loaded into PVA nanofibers, with a specific focus on exploring the neglected potential of catappa leaves. ALE and CLE obtained from the two types of plants can be combined with the PVA. The first medicinal plant was soursop (*Annona muricata linn*), which is considered beneficial for the treatment of cough, asthma, diabetes, heart disease, fever, and cancer (Ilango et al., 2022). Furthermore, the compounds contain annonaceous acetogenins, vitamins, minerals, essential oils, and phytochemicals that have anti-inflammatory and antioxidant properties (Chan et al., 2020). Among the major compounds, acetogenins are most abundant in soursop. Annonaceous acetogenins inhibit the proliferation of the human prostate cancer cell line PC-3 and serve as potential anti-SARS-CoV-2 agents (Prasad et al., 2021). The second medicinal plant is catappa (*Terminalia catappa L*), which can cure diseases such as fever, stomatitis, hypertension, menstrual pain, and bleeding. Catappa contains antifungal and antibacterial agents, as well as other compounds, including alkaloids, tannins, saponins, flavonoids, and terpenoids (Yadav et al., 2021). Antioxidants such as flavonoids, glycosides, and polyphenols can prevent the narrowing of the blood vessels (Mwangi et al., 2024). PVA was successfully combined with ALE and CLE in this study through electrospinning, which is more effective for long-term use. This combination can subsequently be applied in several fields, such as biomedicine and textiles.

2. EXPERIMENTAL SECTION

2.1 Materials

PVA (M_w 89,000-98,000) and analytical-grade ethanol were obtained from Sigma Aldrich, Singapore. Additionally, ALE and CLE were purchased from the Laboratory of Integrated Research and Testing (LPPT), Gadjah Mada University, and the aquades were obtained from Onemed, Palembang.

2.2 Methods

The solution was prepared by mixing 10% (wt%) PVA, CLE, and ALE using aquadest and ethanol as solvents (1:1 ratio) at 60°C and a centrifugation speed of 250 rpm until a homogeneous state was achieved. The resulting solution was referred to as PAC (PVA/ALE/CLE), and the sample percentage ratios are shown in Table 1. The composite solution was transferred into a 10 mL syringe for the electrospinning process using the Labscale Electrospinning Unit NLI601ES (Malaysia). The process was carried out for approximately 12 hours with parameters including an applied voltage of 16.5 kV, a flow rate of 0.2 mL/h, a tip-to-collector distance of 100 mm, and a drum speed of 160 rpm.

Table 1. Comparison of Percentage Ratios in PAC Samples

Sample	PVA (wt%)	Extract (wt%)
PAC-1	10	3
PAC-2	10	4
PAC-3	10	5

2.3 Materials Characterization

The morphology and diameter of the nanofibers were characterized using an AxiaChemiSEM device at a magnification of 5000x. The average diameter was analyzed using the ImageJ software by randomly measuring 100 points on each fiber and preparing graphs using OriginLab Pro 2018. FTIR analysis was conducted to identify the functional groups present in each sample. Furthermore, characterization was carried out using a Shimadzu Type IR Prestige-2, EU, with a wavenumber range of 3500-500 cm^{-1}. Tensile test analysis was conducted to determine the mechanical properties of the samples, including stress-strain, flexibility, and elastic modulus. Characterization was performed using a ZwickRoell UTM tensile testing machine according to ASTM D638 standards.

3. RESULTS AND DISCUSSION

3.1 Scanning Electron Microscope (SEM)

Each sample of the composite membrane produced a smooth surface with a yellowish-brown color, as shown in Figure 1. The results showed a significant change in the distribution and size of the fibers caused by the increased extract concentration. Figure 1(a) shows the average diameter of PAC-1 fibers as 962 ± 378 nm, with the resulting nanofibers being brownish-green and thin. The PAC-2 sample had an average diameter of 1093 ± 327 nm, which is higher than that of PAC-1. A higher extract concentration is an important factor for the increase in diameter (Almafie et al., 2020). An increase in the average diameter also occurred in PAC-3 at 1323 ± 414 nm because the PVA matrix contained more extract (Sofi et al., 2020). The added concentration of the natural leaf extract enhanced the solution viscosity and affected the solution flow during the electrospinning process, producing bead-free nanofibers (Chin and Ng, 2020). The solution stability led to the formation of uniform fibers and increased the average diameter. The use of an ethanol solvent is an important factor in the electrospinning of nanofibers because it helps minimize the narrowing of the solution flow at the needle hole during the process (Ajith et al., 2023).

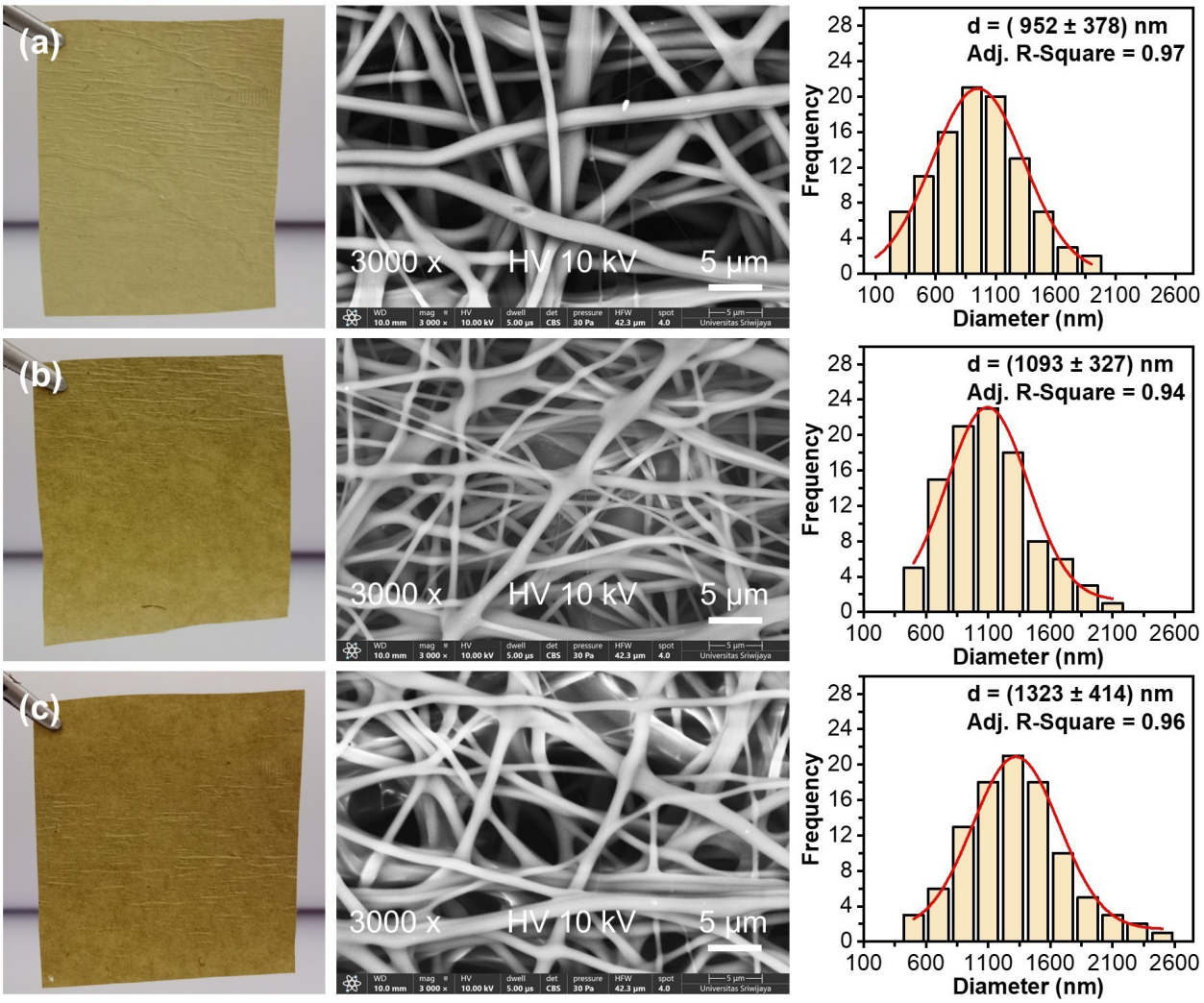

Figure 1. Average Diameter and Fiber Yield of (a) PAC-1, (b) PAC-2, and (c) PAC-3

3.2 Fourier Transform Infrared (FTIR)

FTIR analysis was conducted to determine the functional groups present in each sample. The FTIR spectra showing the absorption peaks for all samples are presented in Figure 2. The FTIR analysis was started with the use of ALE (Figure 2a) to identify the active compounds present in the extract. The initial broad peak in the range of 3400-3200 cm^{-1} corresponds to symmetric −NH stretching of aliphatic amine groups. Peaks at 2924 cm^{-1} and 1735 cm^{-1} suggest the presence of −CH stretching from alkane groups and C=O stretching from carbonyl groups, respectively (de Andrade et al., 2021). Both peaks originate from compounds, such as carboxylic acids or esters, with moderate intensities. Hydroxyl groups, phytochemicals, and alcohol groups are present at 1450 cm <>^{1} B- and are associated with flavonoids or phenols in ALE (Akinsiku et al., 2023). Additionally, ALE contributes to −OH and C=O groups in the -CN amine group stretching observed at the 1250-1020 cm^{-1} range (Shanmugam et al., 2024). The presence of these absorption peaks confirms the presence of bioactive components, such as flavonoids, tannins, and phenolic compounds, which are the primary characteristics of ALE.

CLE showed absorption peaks (Figure 2b) that were largely similar to those of ALE. The initial broad peak in the range of 3400-3200 cm^{-1} signifies the presence of hydroxyl (−OH) groups (Ray et al., 2023). The lower intensity of the peaks suggested differences in the concentrations of phenolic or flavonoid compounds between CLE and ALE. The peak at 1712 cm <ds >^{1} represents the presence of carbonyl (C=H) groups with strong intensity, probably due to gallic acid or other polyphenolic compounds. The bending vibrations of −CH and stretching vibrations of −CO were observed at 1435 cm^{-1} and 1064 cm^{-1}, respectively, signifying the presence of alkane and ester groups (Shanmugam et al., 2020). These peaks confirmed the high content of bioactive compounds, such as flavonoids, tannins,

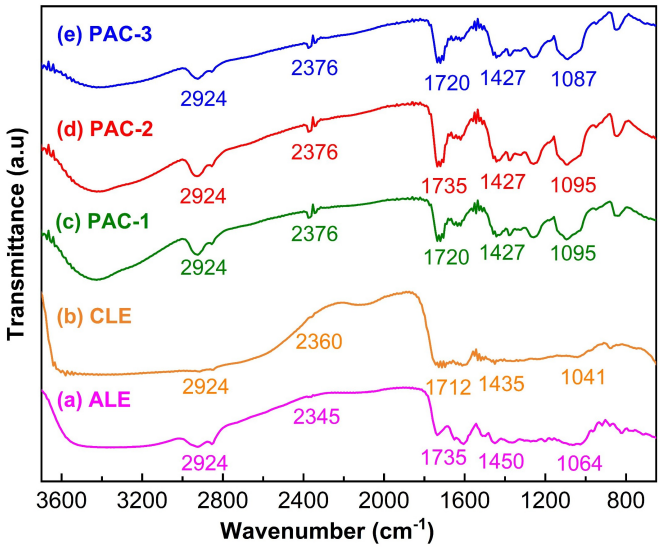

Figure 2. FTIR Spectra of Extract (a) ALE, (b) CLE and Membrane Samples of PVA/ALE/CLE Composite of (b) PAC-1 (c) PAC-2, and (e) PAC-3

and phenolic compounds, in CLE.

The FTIR spectra of the PAC nanofiber membranes (Figure 2c-e) show functional group changes due to the presence of PVA and the ALE/CLE mixture. The broad peaks for each sample are observed in the range of 3500-3220 cm^{-1}, corresponding to −OH hydroxyl stretching dominated by PVA molecules (Almafie et al., 2020). The appearance of hydroxyl groups in the samples suggests the formation of hydrogen bonds with water molecules, which is associated with the hydrophilic nature of PVA (Alfikro et al., 2024). The initial peaks differed slightly between the extracts and were related to the increased ALE/CLE concentration. At the 2924 cm^{-1} peak, −CH stretching from alkane groups occurred because of the molecular structure interaction between PVA and ALE (Rizwana et al., 2021). In the range of 2400-2000 cm^{-1}, CO_2 is adsorbed by the PVA polymer due to the surrounding air and molecules contained in the samples were not released (Haleem et al., 2022). In PAC-1 (Figure 2c), PAC-2 (Figure 2d), and PAC-3 (Figure 2e), ALE/CLE was detected with strong C=O stretching from carboxylic acid compounds. The bending vibrations of −CH in the samples represent the presence of phenolic compounds in each extract (Mwangi et al., 2024).

All three samples showed that the addition of the extract caused interactions between PVA and ALE/CLE, originating from the active compounds in the plant. Increasing the extract concentration disrupts hydrogen bonding, forming new bonds in hydroxyl groups (Kumar et al., 2021). Additionally, carbonyl groups interact with hydroxyl groups via hydrogen bonding, leading to a shift in the wavenumber of C=O stretching (Bhat et al., 2022). At a higher concentration, the observed shift was more pronounced, indicating a more significant interaction between the carbonyl groups and PVA, ALE, and CLE. The active compounds in each extract, such as flavonoids, tannins, and saponins, contain hydroxyl, carbonyl, and ester groups, which interact with the PVA hydroxyl groups through hydrogen bonding

3.3 X-Ray Diffraction (XRD)

X-Ray Diffraction (XRD) analysis of the PAC nanofiber membranes identified a variety of peaks. As illustrated in Figure 3, these peaks suggest that the samples possess an amorphous structure. In the sample using 3% extract (PAC-1), diffraction peaks were identified at 13.64° (031), 16.84° (130), and 19.56° (131), indicating an interaction between the natural extract and PVA polymer (Annu et al., 2021). The diffraction pattern in PAC-2 changed with peak shifts at 14.44° (110), 16.82° (110), and 19.44° (121) due to changes in the polymer structure with the addition of the extract. Increasing the extract concentration can improve the crystal structure of the nanofibers, as indicated by changes in the level of crystallinity in the form of an increase in the intensity and position of the sample diffraction peaks (Abdelghany et al., 2019). However, excessive extract addition tended to damage the regularity of the crystal structure. PAC-3, with a diffraction peak at 19.58° (111), suggests significant potential for amorphous phase redistribution. The addition of 5% extract to the PVA structure led to decreased crystallinity and increased concentration (Annu et al., 2021). This indicates that the addition of ALE/CLE can further reduce the reliability of the PAC polymer matrix (Hafid et al., 2021). The presence of a wide and flat amorphous peak in PAC-3 represents miscibility at the molecular and structural levels owing to strong interactions through hydrogen bonds (Khan et al., 2023).

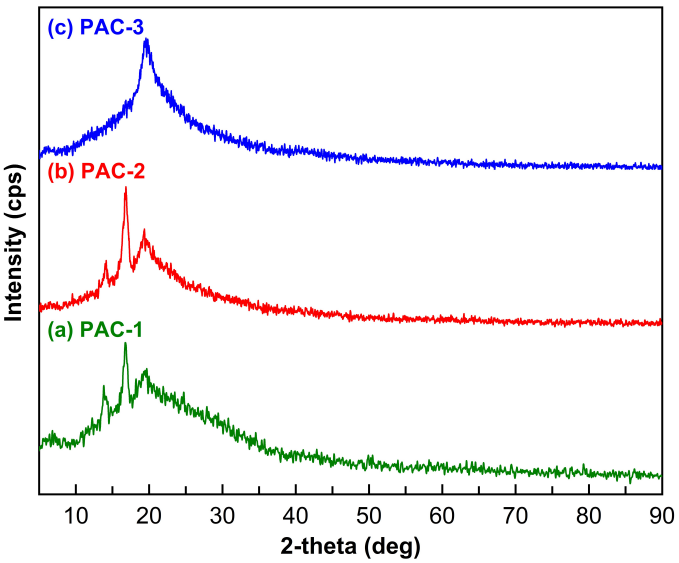

Figure 3. Peak Diffraction of Changes in the Crystal Structure of PVA Nanofiber Membranes (a) PAC-1, (b) PAC-2, and (c) PAC-3.

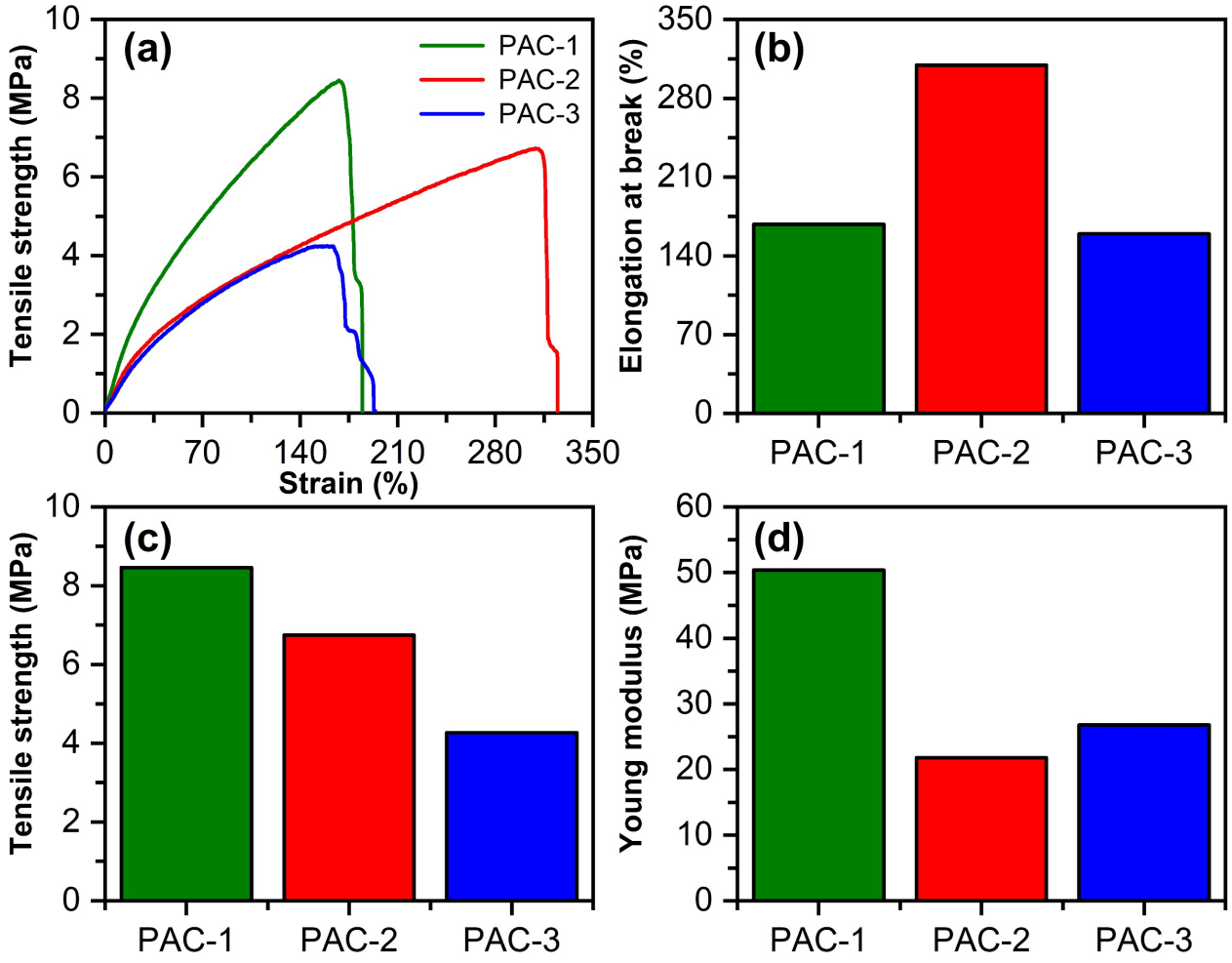

Figure 4. Mechanical Properties of PAC Membrane Composite Nanofibers: (a) Stress-Strain Curve, (b) Elongation, (c) Tensile Strength, And (d) Young's Modulus.

Table 2. Antibacterial Inhibition Zone Activity of Pure Extract and PAC Nanofiber Membrane Samples Against Gram-Positive (*S. aureus*) and Gram-Negative (*P. aeruginosa*) Bacteria.

Bacteria	Zone of Inhibition (mm)				
	ALE	CLE	PAC-1	PAC-2	PAC-3
Staphylococcus aureus	12.3	16.8	9.8	12.1	14.4
Pseudomonas aeruginosa	13.0	13.1	8.0	8.8	11.3

3.4 Tensile Test

A tensile strength mechanical test was conducted to evaluate the mechanical strength of the nanofibers for proper application in various fields. Graphs of the tensile stress-strain and Young's modulus results are shown in Figure 4. Nanofibers require good mechanical properties for various medical applications. Stress–strain curves and correlational analysis of the three nanofibers. Samples PAC-1, PAC-2, and PAC-3 have tensile strength (σ) 8.46, 6.74, and 4.27 MPa, with the elongation at break (ϵ) of 180%, 330%, and 192%, as well as Young's modulus (E) of 20.2 ± 180% MPa, 6.34 ± 330% MPa, and 0.89 ± 192% MPa, respectively. An increase in the diameter of the nanofibers caused a decrease in the tensile strength. The interaction between hydrogen bonds alters the molecular weight of PVA, leading to differences in the Young's modulus values (Bazzi et al., 2022), while each sample has varying ϵ values. The extract concentration influenced the results obtained, with relatively low samples, such as PAC-1, being dominated by PVA properties. As the concentration increases, as in PAC-2, the interaction between PVA hydrogen bonds and the extract enhances tissue flexibility. However, PAC-3, with a very high extract concentration, disrupts the PVA network and initiates changes in the microstructure, which can reduce the stretchability. The reduction in tensile strength following ALE/CLE addition is related to the aggregation of several areas of nanofibers, which act as stress concentration points and prevent load/stress

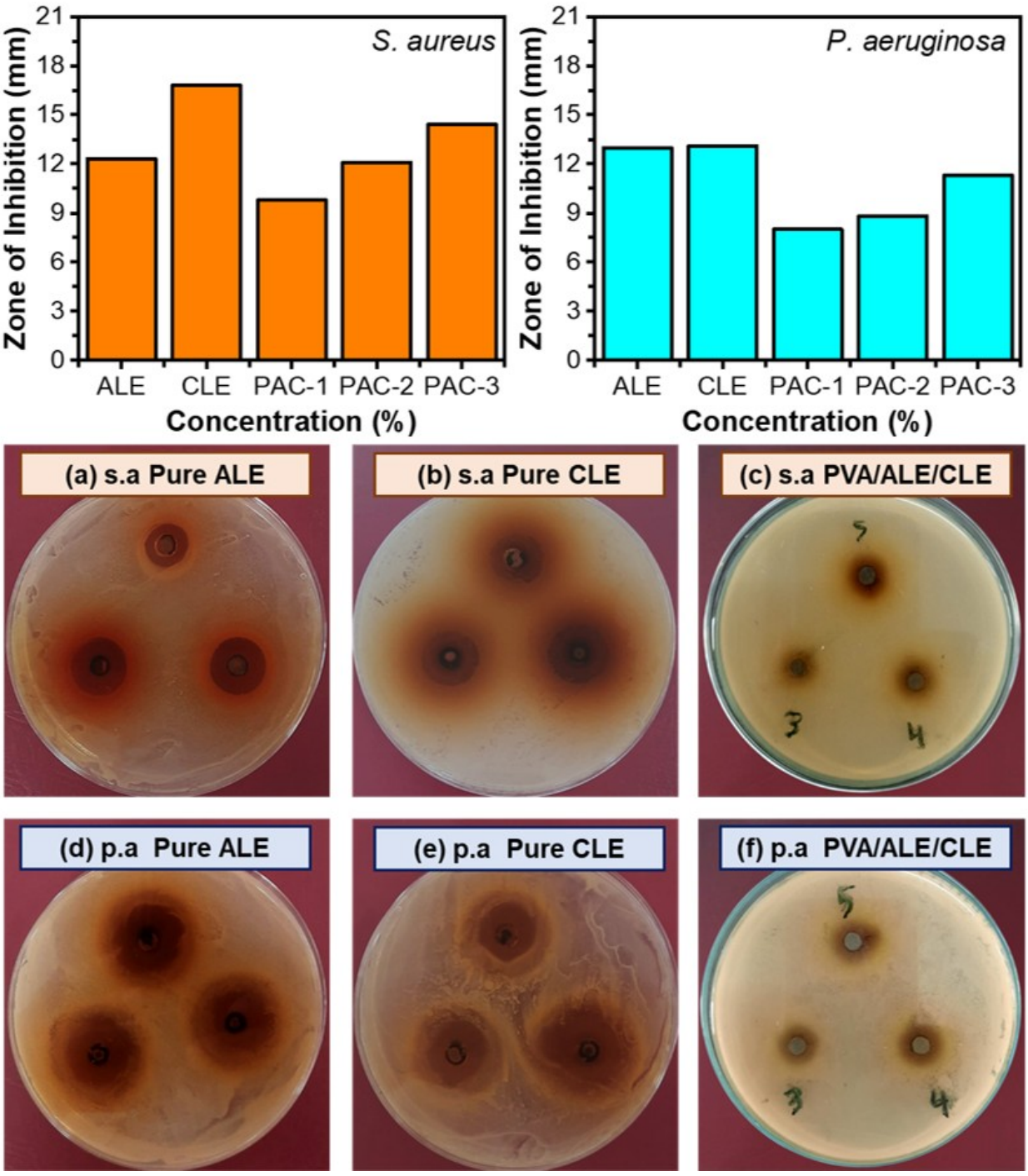

Figure 5. Antibacterial Activity Against Gram-Positive Bacteria (*S. aureus*), (a) Pure ALE; (b) Pure CLE; (c) PAC, and Gram-Negative Bacteria (*P. aeruginosa*), (d) Pure ALE; (e) Pure CLE; (f) PAC, PAC-1 is 3, PAC-2 is 4, and PAC-3 is 5.

transfer (Lv et al., 2021). The weakening of intermolecular interactions in the polymer can leave space for the rearrangement of chains, thereby increasing the surface area of the fibers. The mechanical properties of the samples were influenced by the chemical structure and molecular weight of the PVA chain (Nikbakht et al., 2020). The energy required for the deformation of nanofibers is less because of the decrease in the network density in the PVA matrix, leading to a significantly reduced tensile strength value (Xu et al., 2021).

Table 3. Comparative Analysis of Antibacterial Inhibition Zone Diameters Among Various Extract Samples. (+) is Composite Content

Material	Bacteria	Extract solvent	Max. inhibition zone (mm)	Ref.
ALE	*E. coli*	Ethanol	17.00	(Jemikalajah et al., 2021)
ALE	*P. aeruginosa*	Ethanol	17.00	(Jemikalajah et al., 2021)
ALE	*Salmonella*	Methanol	8.00	(Ngemenya et al., 2022)
CLE	*S. aureus*	Ethanol	30.07	(Dewi and Mardhiyani, 2021)
CLE	*S. epidermis*	Ethanol	19.17	(Dewi and Mardhiyani, 2021)
CLE	*E. coli*	Ethanol	8.00	(Dewi and Mardhiyani, 2021)
CLE	*S. aureus*	Ethanol	13.30	(Orillaneda et al., 2022)
Ag-NPs + CLE	*S. aureus*	De-ionized water	12.13	(Ansari et al., 2021)
Ag-NPs + CLE	*P. aeruginosa*	De-ionized water	20.20	(Ansari et al., 2021)
Ag-NPs + CLE	*C. albicans*	De-ionized water	15.03	(Ansari et al., 2021)
PVA+ALE + CLE	*S. aureus*	Ethanol	14.40	This study
PVA+ ALE + CLE	*P. aeruginosa*	Ethanol	11.30	This study

3.5 Antibacterial Activity

The test results in Figure 5 show an increase in the inhibition zone (ZoI) of each sample tested. In the PAC-1, PAC-2, and PAC-3 samples, there was a significant increase in gram-positive bacteria (*S. aureus*) (Figures 5 a-c) and gram-negative bacteria (*P. aeruginosa*) (Figures 5d-f). Significant inhibition effects were observed for the diameters of the inhibition zones of *S. aureus* and *P. aeruginosa*. Active compounds such as flavonoids found in ALE produce antibacterial effects by disrupting bacterial wall integrity, leading to cell leakage and death (Campos et al., 2023). Phytochemicals, including flavonoids and phenolic acids, abundantly present in CLE often damage the cell wall to achieve bacterial inhibition (Madhavan et al., 2023). In this study, the inhibition zone diameters of PAC nanofiber membrane samples were positively correlated with ALE/CLE content, and the samples could prevent bacterial colonization. Figures 5a and 5e confirm that there is damage to the cell walls of gram-positive and gram-negative bacteria that can inhibit bacteria. This is consistent with the significant increase in the diameter of the barrier zone of each sample.

The antibacterial properties of each sample were evaluated by directly observing the growth of *P. aeruginosa* (p.a) and *S. aureus* (s.a) on the culture plates. The nanofiber membrane samples had significant inhibitory effects on these two bacteria, as shown in Table 2. The antibacterial test on gram-positive *S. aureus* produced samples of various categories. The inhibition zone diameter for pure ALE was found to be 12.3 mm, and that for pure CLE was 16.8 mm, both of which fell into the strong category. In the extract incorporated into PAC nanofiber membranes, the inhibition zone diameters varied. The PAC-1 sample showed moderate antibacterial properties, with an inhibition zone of 9.8 mm. Meanwhile, PAC-2 and PAC-3 had inhibition zones of 12.1 mm and 14.4 mm, respectively, both classified as strong. These results correspond with studies conducted by Akanji (2023) on ALE, and Bouagnon et al. (2024) on CLE, which showed moderate antibacterial activity against *S. aureus*. In the pure extract samples, gram-negative *P. aeruginosa* had slightly larger inhibition zone diameters than gram-positive *S. aureus*. PAC-1 produced an inhibition zone of 8.0 mm, while PAC-2 had an inhibition zone of 8.8 mm, both of which were classified as moderate. The inhibition zone diameter of PAC-3 increased to 11.3 mm, leading to its positioning in the strong category. Antibacterial studies by Rumanti et al. (2020) on ALE and Darmawati et al. (2023) classified the extract as strong, with CLE showing the highest inhibition zone. The ALE/CLE combination generated an average inhibition zone that was classified as strong.

Table 3 shows a comparison of the antibacterial inhibition zone diameters between the various extract samples. Previous studies generally categorized the inhibition zones for ALE and CLE in the strong to very strong range. This phenomenon can be associated with gram-positive bacteria comprising cytoplasmic membranes beneath a thick peptidoglycan wall with many pores, which promotes greater susceptibility to signal delivery into the cell (Tavares et al., 2020). However, gram-negative bacteria have a complex cell wall structure with a peptidoglycan layer between the outer and cytoplasmic membranes, reducing their susceptibility to molecular attacks (Avila-Calderón

et al., 2021). Nanofibers can adhere to gram-positive bacteria and cause disruptions in the cell, leading to higher inhibition zones for *S. aureus* than for gram-negative *P. aeruginosa*. The inhibition zone activity in PAC-1, PAC-2, and PAC-3 was due to the presence of antibacterial secondary metabolites, including flavonoids, tannins, and saponins, as explained by the FTIR analysis. The nanofibers in all PAC samples exhibited enhanced antibacterial activity owing to the ALE/CLE extract content. The extract combination was found to cause damage to bacterial surfaces, cell leakage, and death. Additionally, the samples contained extracts with superior antibacterial properties that disrupted the bacterial wall permeability and cell respiration.

4. CONCLUSIONS

In conclusion, this study successfully spun and characterized homogeneous PAC nanofiber membranes. The results showed that increasing the extract concentration increased the diameter of the nanofibers produced. In addition, the stability of the spinning process contributes to the formation of uniform fibers. The ALE/CLE functional groups and PAC nanofiber membranes in the FTIR spectra exhibited nearly identical absorption peaks. PVA dominated the PAC-1 sample, whereas increasing the extract concentration led to more active compounds in PAC-2 and PAC-3. The increase in fiber diameter and the formation of new hydrogen bonds in the hydroxyl groups decreased the tensile strength of the fibers (θ) from 8.46 MPa to 4.27 MPa. The chemical structure and molecular weight of the PVA chains affect the mechanical properties of the produced samples. Antibacterial analysis showed superior antibacterial properties, as evidenced by the formation of inhibition zones against *S. aureus* and *P. aeruginosa* in the moderate-to-strong category. The increase in the inhibition zone diameters, ranging from 9.8–14.4 nm (*S. aureus*) and 8.0–11.3 nm (*P. aeruginosa*), signified the presence of secondary metabolites in the extract, such as flavonoids, tannins, and saponins. This study suggests PAC nanofiber membranes as a potential alternative, offering new insights into the characteristics of PVA combined with ALE/CLE, leading to its suitability for applications in biomedicine and textiles.

5. ACKNOWLEDGMENT

This study was fully supported by the Ministry of Education, Culture, Research, and Technology of the Indonesia-Fundamen tal Research Scheme Group in the Focus Area of Advanced Materials (contract number 090/E5/PG.02.00).PL/2024 and decree number 0459/E5/PG.02.00/2024.

REFERENCES

Abdelghany, A. M., A. A. Menazea, and A. M. Ismail (2019). Synthesis, Characterization and Antimicrobial Activity of Chitosan/Polyvinyl Alcohol Blend Doped with *Hibiscus Sabdariffa L.* Extract. *Journal of Molecular Structure*, **1197**; 603–609

Ajith, G., G. P. Tamilarasi, G. Sabarees, S. Gouthaman, K. Manikandan, V. Velmurugan, V. Alagarsamy, and V. R. Solomon (2023). Recent Developments in Electrospun Nanofibers as Delivery of Phytoconstituents for Wound Healing. *Drugs and Drug Candidates*, **2**(1); 148–171

Akanji, O. C. (2023). Antibacterial Activity of *Annona muricata* Leaves' Extracts. *International Journal of Frontline Research in Science and Technology*, **2**(1); 024–028

Akinsiku, A. A., R. O. Odaudu, O. C. De Campos, A. O. Adeyemi, and O. Ejilude (2023). Synthesis of Low Toxic Silver-Cobalt Nanoparticles Using *Annona muricata* Leaf Extract: Antimicrobial Evaluation. *Inorganic Chemistry Communications*, **153**; 110837

Akpan, U. M., M. Pellegrini, A. A. Salifu, J. D. Obayemi, T. Ezenwafor, D. Browe, C. J. Ani, Y. Danyuo, S. Dozie-Nwachukwu, O. S. Odusanya, J. Freeman, and W. O. Soboyejo (2021). In Vitro Studies of *Annona muricata L.* Extract-Loaded Electrospun Scaffolds for Localized Treatment of Breast Cancer. *Journal of Biomedical Materials Research - Part B Applied Biomaterials*, **109**(12); 2041–2056

Al-Abduljabbar, A. and I. Farooq (2023). Electrospun Polymer Nanofibers: Processing, Properties, and Applications. *Polymers*, **15**(1); 65

Alfikro, I., Jorena, O. C. Satya, E. Koriyanti, F. Monado, and I. Royani (2024). Assessment of Different Crosslinking Mechanisms on PVA-Based Membranes to Achieve Water Resistance with Iron Imprinting Sites. *Chimica Techno Acta*, **11**(3); 6–13

Almafie, M. R., R. Dani, Riyanto, L. Marlina, J. Jauhari, and I. Sriyanti (2024). Preparation of PAN/PVDF Nanofiber Mats Loaded with Coconut Shell Activated Carbon and Silicon Dioxide for Lithium-Ion Battery Anodes. *Science and Technology Indonesia*, **9**(2); 427–447

Almafie, M. R., A. Fudholi, R. Dani, M. K. N. A. Idjan, I. Royani, and I. Sriyanti (2025). Effects of Electrospinning Parameters on Polycaprolactone Membrane Diameter: An Investigation Utilizing Central Composite Design and Characterization. *Results in Engineering*, **25**; 104002

Almafie, M. R., Z. Nawawi, J. Jauhari, and I. Sriyanti (2020). Electrospun of Poly (Vinyl Alcohol)/Potassium Hydroxide (PVA/KOH) Nanofiber Composites Using the Electrospinning Method. *IOP Conference Series: Materials Science and Engineering*, **850**(1); p. 012051

Annu, A. Ali, and S. Ahmed (2021). Eco-Friendly Natural Extract Loaded Antioxidative Chitosan/Polyvinyl Alcohol Based Active Films for Food Packaging. *Heliyon*, **7**(3); e06550

Ansari, M. A., A. Kalam, A. G. Al-Sehemi, and M. N. Alomary (2021). Counteraction of Biofilm Formation and Antimicrobial Potential of *Terminalia catappa* Functionalized Silver Nanoparticles against *Candida albicans* and Multidrug-Resistant Gram-Negative and Gram-Positive Bacteria. *Antibiotics*, **10**; 1–21

Avila-Calderón, E. D., M. d. S. Ruiz-Palma, M. G. Aguilera-Arreola, N. Velázquez-Guadarrama, E. A. Ruiz, Z. Gomez-

Lunar, S. Witonsky, and A. Contreras-Rodríguez (2021). Outer Membrane Vesicles of Gram-Negative Bacteria: An Outlook on Biogenesis. *Frontiers in Microbiology*, **12**; 557902

Bazzi, M., I. Shabani, and J. A. Mohandesi (2022). Enhanced Mechanical Properties and Electrical Conductivity of Chitosan/Polyvinyl Alcohol Electrospun Nanofibers by Incorporation of Graphene Nanoplatelets. *Journal of the Mechanical Behavior of Biomedical Materials*, **125**; 104975

Bhat, V. G., S. S. Narasagoudr, S. P. Masti, R. B. Chougale, A. B. Vantamuri, and D. Kasai (2022). Development and Evaluation of Moringa Extract Incorporated Chitosan/Guar Gum/Poly (Vinyl Alcohol) Active Films for Food Packaging Applications. *International Journal of Biological Macromolecules*, **200**; 50–60

Bouagnon, J. J. R., Y. Konan, K. I. Sinan, F. Konan, G. E. K. Bolou, L. R. Koffi, D. Yeo, J. D. N'Guessan, G. Zengin, A. J. Djaman, M. A. Yılmaz, and M. Dosso (2024). In Vitro Research to Evaluate the Antioxidant Effects, Inhibiting Enzymes, Methicillin-Resistant *Staphylococcus aureus* Strains of *Terminalia catappa* Extracts. *Scientific African*, **23**; e02058

Campos, L. M., A. S. O. Lemos, I. O. M. Diniz, L. A. Carvalho, T. P. Silva, P. R. B. Dib, E. D. Hottz, L. M. Chedier, R. C. N. Melo, and R. L. Fabri (2023). Antifungal *Annona muricata L.* (Soursop) Extract Targets the Cell Envelope of Multi-Drug Resistant Candida Albicans. *Journal of Ethnopharmacology*, **301**; 115856

Chan, W. J. J., A. J. McLachlan, J. R. Hanrahan, and J. E. Harnett (2020). The Safety and Tolerability of *Annona muricata* Leaf Extract: A Systematic Review. *Journal of Pharmacy and Pharmacology*, **72**(1); 1–16

Chin, C. Y. and S. F. Ng (2020). Development of Moringa Oleifera Standardized Leaf Extract Nanofibers Impregnated onto Hydrocolloid Film as a Potential Chronic Wound Dressing. *Fibers and Polymers*, **21**(11); 2462–2472

Darmawati, S., L. Kurniasih, H. N. A. Safitri, B. S. Pratomo, and M. E. Prastiyanto (2023). Antibacterial Activity of Ketapang (*Terminalia cattapa L.*) Leaf Extract against *Staphylococcus aureus and Pseudomonas aeruginosa* Isolates of Diabetic Wounds. In *Proceedings of the First International Conference on Medical Technology (ICoMTech 2021)*, volume 1. Atlantis Press International BV, pages p. 93–101

de Andrade, F. H. D., R. S. de Araújo Batista, T. B. L. Melo, F. H. A. Fernandes, R. O. Macedo, F. S. de Souza, and A. G. Wanderley (2021). Characterization and Compatibility of Dry Extract from *Annona muricata L.* and Pharmaceutical Excipients. *Journal of Thermal Analysis and Calorimetry*, **143**(1); 237–246

Dewi, A. P. and D. Mardhiyani (2021). Formulation and Antibacterial Activity of Liquid Soap Containing Ketapang *(Terminalia catappa L.)* Leaves Extract. *Borneo Journal of Pharmacy*, **4**(1); 43–50

Gheibi, P., N. Jabbari, N. K. Alghari, S. M. Nesaei, R. Farhoudi, and Z. Eftekhari (2024). Electrospun PVA Nanofibers Loaded with Antimicrobial Herbal Extracts for Healing the Infectious Wound. *Jundishapur Journal of Natural Pharmaceutical Products*, **19**(1); 1–10

Hafid, H. S., F. N. Omar, J. Zhu, and M. Wakisaka (2021). Enhanced Crystallinity and Thermal Properties of Cellulose from Rice Husk Using Acid Hydrolysis Treatment. *Carbohydrate Polymers*, **260**; 117789

Haleem, N., A. Khattak, Y. Jamal, M. Sajid, Z. Shahzad, and H. Raza (2022). Development of Poly Vinyl Alcohol (PVA) Based Biochar Nanofibers for Carbon Dioxide CO_2 Adsorption. *Renewable and Sustainable Energy Reviews*, **157**; 112019

Ilango, S., D. K. Sahoo, B. Paital, K. Kathirvel, J. I. Gabriel, K. Subramaniam, P. Jayachandran, R. K. Dash, A. K. Hati, T. R. Behera, P. Mishra, and R. Nirmaladevi (2022). A Review on *Annona muricata* and Its Anticancer Activity. *Cancers*, **14**(18); 1–31

Jemikalajah, J., F. O. Enwa, and E. C. Chiedozie (2021). Antibacterial Activity of Annona Muricata (Soursop) Leaf Extract on *Escherichia coli and Pseudomona aeruginosa*. *Turkish Journal of Physiotherapy and Rehabilitation*, **32**(3); 13918–13923

Keirouz, A., Z. Wang, V. S. Reddy, Z. K. Nagy, P. Vass, M. Buzgo, S. Ramakrishna, and N. Radacsi (2023). The History of Electrospinning: Past, Present, and Future Developments. *Advanced Materials Technologies*, **8**(11); 1–34

Khan, A. K., S. Kaleem, F. Pervaiz, T. A. Sherazi, S. A. Khan, F. A. Khan, T. Jamshaid, M. I. Umar, W. Hassan, M. Ijaz, and G. Murtaza (2023). Antibacterial and Wound Healing Potential of Electrospun PVA/MMT Nanofibers Containing Root Extract of Berberis Lycium. *Journal of Drug Delivery Science and Technology*, **79**; 103987

Kumar, P., R. Tanwar, V. Gupta, A. Upadhyay, A. Kumar, and K. K. Gaikwad (2021). Pineapple Peel Extract Incorporated Poly(Vinyl Alcohol)-Corn Starch Film for Active Food Packaging: Preparation, Characterization and Antioxidant Activity. *International Journal of Biological Macromolecules*, **187**; 223–231

Lv, H., S. Cui, Q. Yang, X. Song, D. Wang, J. Hu, Y. Zhou, and Y. Liu (2021). AgNPs-Incorporated Nanofiber Mats: Relationship Between AgNPs Size/Content, Silver Release, Cytotoxicity, and Antibacterial Activity. *Materials Science and Engineering C*, **118**; 111331

Madhavan, K., Y. Rukayadi, and N. A. A. Mutalib (2023). Phytochemical Constituents and Toxicity Analysis of Ethanolic Ketapang *(Terminalia catappa L.)* Leaf Extract. *Malaysian Applied Biology*, **52**(3); 105–114

Mwangi, W. C., W. Waudo, M. E. Shigwenya, and J. Gichuki (2024). Phytochemical Characterization, Antimicrobial and Antioxidant Activities of *Terminalia catappa* Methanol and Aqueous Extracts. *BMC Complementary Medicine and Therapies*, **24**(1); 1–11

Ngemenya, M. N., R. Asongana, D. Zofou, R. A. Ndip, L. O. Itoe, and S. B. Babiaka (2022). In Vitro Antibacterial Potential Against Multidrug-Resistant Salmonella, Cytotoxicity, and Acute Biochemical Effects in Mice of Annona Muricata Leaf Extracts. *Evidence-Based Complementary and Alternative Medicine*, **2022**(1); 3144684

Nikbakht, M., M. Salehi, S. M. Rezaya, and R. F. Majidi (2020). Various Parameters in the Preparation of Chitosan/Polyethylene Oxide Electrospun Nanofibers Containing Aloe Vera Extract for Medical Applications. *Nanomedicine Journal*, **7**(1); 21–28

Orillaneda, K. N. O., E. S. Caracal, I. D. E. A. D. Campo, A. K. T. Flores, L. M. Malda, C. E. B. Morales, and C. J. D. Reniedo (2022). Phytochemical Screening, Antioxidant, and Antibacterial Property of Talisay *(Terminalia catappa)* Leaves Ethanolic Extract Against *Staphylococcus aureus* Used as Formulated Ointment. *International Journal of Pharma Medicine and Biological Sciences*, **11**(4); 89–95

Prasad, S. K., S. Pradeep, C. Shimavallu, S. P. Kollur, A. Syed, N. Marraiki, C. Egbuna, M. A. Gaman, O. Kosakowska, W. C. Cho, K. C. Patrick-Iwuanyanwu, J. Ortega Castro, J. Frau, N. Flores-Holguín, and D. Glossman-Mitnik (2021). Evaluation of *Annona muricata* Acetogenins as Potential Anti-SARS-CoV-2 Agents Through Computational Approaches. *Frontiers in Chemistry*, **8**; 1–7

Ray, L., M. Das, and J. Tripathy (2023). *Terminalia catappa* Leaf Extract Mediated Eco-Friendly Synthesis of Cerium Oxide Nanoparticles. *Materials Today: Proceedings*

Rizwana, H., N. A. Bokahri, S. A. Alsahli, A. S. Al Showiman, R. M. Alzahrani, and H. A. Aldehaish (2021). Postharvest Disease Management of Alternaria Spots on Tomato Fruit by *Annona muricata* Fruit Extracts. *Saudi Journal of Biological Sciences*, **28**(4); 2236–2244

Rumanti, R. M., M. Rimala, I. Efendy, I. Ginting, Y. Bess, C. Simarmata, and V. E. Diana (2020). The Comparison of Antibacterial Activities of Soursop Leaf *(Annona muricata L.)* and Basil Leaf *(Ocimum americanum L.)* Ethanolic Extracts on Gel Formulated Against *Staphilococcus aureus* and Propionibacterium Acnes. *Asian Journal of Pharmaceutical Research and Development*, **8**(4); 1–4

Sapalidis, A. A. (2020). Porous Polyvinyl Alcohol Membranes: Preparation Methods and Applications. *Symmetry*, **12**(6); 960

Sen, S., T. Bal, and A. D. Rajora (2022). Green Nanofiber Mat from HLM–PVA–Pectin (Hibiscus Leaves Mucilage–Polyvinyl Alcohol–Pectin) Polymeric Blend Using Electrospinning Technique as a Novel Material in Wound-Healing Process. *Applied Nanoscience (Switzerland)*, **12**(2); 237–250

Shanmugam, H., B. K. Biswal, S. Sundaresan, D. Selvakumar, Z. J. Kennedy, and R. S. Priya (2024). Comparative Nutrient and Chemometric Analysis of Leaf to Fruits of Sourpsop *(Annona muricata)* and Bullock's Heart *(Annona reticulata)*: Implications for Nutraceutical Development. *Journal of Food Composition and Analysis*, **135**; 106686

Shanmugam, K. . B., S. Rangaraj, K. Subramani, S. Srinivasan, W. K. Aicher, and R. Venkatachalam (2020). Biomimetic TiO_2-Chitosan/Sodium Alginate Blended Nanocomposite Scaffolds for Tissue Engineering Applications. *Materials Science and Engineering C*, **110**; 110710

Sofi, H. S., R. Rashid, T. Amna, R. Hamid, and F. A. Sheikh (2020). Recent Advances in Formulating Electrospun Nanofiber Membranes: Delivering Active Phytoconstituents. *Journal of Drug Delivery Science and Technology*, **60**; 102038

Sriyanti, I., R. Dani, M. R. Almafie, R. U. Partan, M. K. N. Ap Idjan, and L. Marlina (2024). Optimization of Diameter and Mechanical Properties of Polyacrylonitrile/ Polyvinylidene Fluoride/ Graphene Oxide Coconut Shell Composite Nanofiber Mats with Using Response Surface Methodology. *Case Studies in Chemical and Environmental Engineering*, **10**; 101030

Tavares, T. D., J. C. Antunes, J. Padrão, A. I. Ribeiro, A. Zille, M. T. P. Amorim, F. Ferreira, and H. P. Felgueiras (2020). Activity of Specialized Biomolecules Against Gram-Positive and Gram-Negative Bacteria. *Antibiotics*, **9**(6); 1–16

Valipouri, A., A. Alsikh, and Z. Rahimi Dashtlouei (2024). Investigating the Wettability Control of Fluorocarbon-Coated Nanofiber Membranes by Electrowetting Process. *Journal of Electrostatics*, **128**; 103892

Xu, K., Y. Wang, B. Zhang, C. Zhang, and T. Liu (2021). Stretchable and Self-Healing Polyvinyl Alcohol/Cellulose Nanofiber Nanocomposite Hydrogels for Strain Sensors with High Sensitivity and Linearity. *Composites Communications*, **24**; 100677

Yadav, S., R. Kapoor, P. Mittal, and G. Ajmal (2021). *Terminalia catappa Linn.*: A Treasury of Pharmacological Benefits. *Uttar Pradesh Journal of Zoology*, **42**(24); 1386–1396

